Title

Trabecular bone microstructure is impaired in the proximal femur of human immunodeficiency virus-infected men with normal bone mineral density

Journal

Quantitative Imaging in Medicine and Surgery, 8(1)

ISSN

2223-4292

Authors

Kazakia, Galateia J

Carballido-Gamio, Julio

Lai, Andrew

et al.

Publication Date

2018-02-01

DOI

10.21037/qims.2017.10.10

Peer reviewed

Original Article

Trabecular bone microstructure is impaired in the proximal femur of human immunodeficiency virus-infected men with normal bone mineral density

Galateia J. Kazakia[1], Julio Carballido-Gamio[2], Andrew Lai[1], Lorenzo Nardo[1], Luca Facchetti[1], Courtney Pasco[1], Chiyuan A. Zhang[1], Misung Han[1], Amanda Hutton Parrott[1], Phyllis Tien[1], Roland Krug[1]

[1]Department of Radiology and Biomedical Imaging, University of California San Francisco, San Francisco, CA, USA; [2]Department of Radiology, University of Colorado Denver, Denver, CO, USA

Correspondence to: Roland Krug. Department of Radiology and Biomedical Imaging, University of California San Francisco, 185 Berry Street, Suite 350, Campus Box 0946, San Francisco, CA 94107-5705, USA. Email: Roland.Krug@ucsf.edu.

Background: There is evidence that human immunodeficiency virus (HIV) infection and antiretroviral therapy (ART) are independent risk factors for osteoporosis and fracture which is not solely explained by changes in bone mineral density. Thus, we hypothesized that the assessment of trabecular microstructure might play an important role for bone quality in this population and might explain the increased fracture risk. In this study, we have assessed bone microstructure in the proximal femur using high-resolution magnetic resonance imaging (MRI) as well as in the extremities using high resolution peripheral quantitative computed tomography (HR-pQCT) in HIV-infected men and healthy controls and compared these findings to those based on areal bone mineral density (aBMD) derived from dual X-ray absorptiometry (DXA) which is the standard clinical parameter for the diagnosis of osteoporosis.

Methods: Eight HIV-infected men and 11 healthy age-matched controls were recruited and informed consent was obtained before each scan. High-resolution MRI of the proximal femur was performed using fully balanced steady state free precession (bSSFP) on a 3T system. Three volumes of interest at corresponding anatomic locations across all subjects were defined based on registrations of a common template. Four MR-based trabecular microstructural parameters were analyzed at each region: fuzzy bone volume fraction (f-BVF), trabecular number (Tb.N), thickness (Tb.Th), and spacing (Tb.Sp). In addition, the distal radius and distal tibia were imaged with HR-pQCT. Four HR-pQCT-based microstructural parameters were analyzed: trabecular bone volume fraction (BV/TV), Tb.N, Tb.Th, and Tb.Sp. Total hip and spine aBMD were determined from DXA.

Results: Microstructural bone parameters derived from MRI at the proximal femur and from HR-pQCT at the distal tibia showed significantly lower bone quality in HIV-infected patients compared to healthy controls. In contrast, DXA aBMD data showed no significant differences between HIV-infected patients and healthy controls.

Conclusions: Our results suggest that high-resolution imaging is a powerful tool to assess trabecular bone microstructure and can be used to assess bone health in HIV-infected men who show no differences to healthy males by DXA aBMD. Advances in MRI technology have made microstructural imaging at the proximal femur possible. Further studies in larger patient cohorts are clearly warranted.

Keywords: Human immunodeficiency virus (HIV); trabecular bone microstructure; high-resolution magnetic resonance imaging (MRI); high resolution peripheral quantitative computed tomography (HR-pQCT); dual X-ray absorptiometry (DXA); areal bone mineral density (aBMD)

Submitted Aug 22, 2017. Accepted for publication Oct 10, 2017.
doi: 10.21037/qims.2017.10.10
View this article at: http://dx.doi.org/10.21037/qims.2017.10.10

Introduction

Human immunodeficiency virus (HIV) infection and antiretroviral therapy (ART) are established independent risk factors for osteoporosis and elevated prevalence of fracture (1-3) as well as avascular necrosis (AVN) (4,5). Areal bone mineral density (aBMD) derived from dual X-ray absorptiometry (DXA) is the standard clinical parameter for the diagnosis of osteoporosis and assessment of risk of osteoporotic bone fracture (6,7). However, data from 138 HIV-infected women and 402 controls showed an increased incidence of fragility fractures in HIV-infected women despite similar aBMD (8). Another study demonstrated that only four of 11 HIV infected women with fractures were diagnosed as osteoporotic by DXA (9). Thus, increased risk of fracture is not solely explained by aBMD. In addition, bone microstructure might play an important role in the context of bone strength in this population. There is increasing evidence that HIV infection and its treatment are associated with bone quality changes that do not impact BMD but do increase fracture risk.

Data supporting this theory have been reported for the extremities (10,11), however, no study has determined whether central skeletal sites are affected similarly. The proximal femur is an important anatomical site for fracture, and femur fractures are usually accompanied with high morbidity and mortality (12). As HIV-infected individuals live longer through effective ART, HIV-related bone deterioration is superimposed upon age-related bone deterioration and is expected to result in greater rates of fragility fractures than in the general population in the near future (13,14). In addition to the effect of HIV infection, it has been shown that ART exacerbates bone loss (15,16).

In-vivo imaging of the trabecular bone microstructure at the proximal femur with high-resolution magnetic resonance imaging (MRI) is quite challenging due to signal-to-noise constraints and has been accomplished only recently with advanced MR pulse sequences and improved hardware (17). Further progress in the field has now enabled very high spatial resolution in the proximal femur (18,19), which was previously only achieved in the extremities (20-23). In addition, novel coil correction methods (24) and image analysis approaches (25-28) complement the in-vivo assessment of structural bone integrity in the proximal femur. Lastly, the development of advanced image registration techniques allow the comparison of structural bone parameters across a set of MR images at corresponding anatomic locations, e.g., the femoral head, greater trochanter, femoral neck, as well as the total femur (29,30).

The purpose of this study was twofold. First, to apply recently developed MRI methods and post-processing techniques to quantify the trabecular bone microstructure in the proximal femur in anatomically corresponding volumes of interest across HIV-infected subjects and uninfected controls; second, to compare the MRI results with microstructural assessments of the distal radius and distal tibia using HR-pQCT as well as with aBMD from DXA measurements.

Methods

Subjects

In our main study, 8 HIV-infected men and 11 uninfected control men were included. Informed consent was obtained before scans. HIV-infected participants were recruited from the UCSF Department of Infectious Diseases and the UCSF 360: Positive Care Center. Patients were diagnosed with HIV an average of 10 years prior to enrollment and were on stable long-term ART. Exclusion factors included use of bisphosphonates, thyroid hormone replacement, steroids and illicit drug use. Controls were recruited from the general population and were age-matched to the HIV-infected subjects. All HIV-infected individuals completed the Community Healthy Activities Model Program for Seniors (CHAMPS) Physical Activity Questionnaire for Older Adults. The questionnaire used revised Metabolic Weight Values (MET) to adjust for the older population (31). MET-hours per week (including light, moderate, and vigorous activity levels) were calculated for each HIV-infected individual. In an ancillary study, 20 HIV-infected men and 18 age- and BMI-matched uninfected control men were recruited through the same mechanisms described above and informed consent was obtained. These participants were scanned with HR-pQCT but not MRI or DXA. The purpose of this ancillary study was to obtain more closely BMI-matched groups to investigate whether BMI alone could be driving differences in bone quality between HIV-infected and control individuals.

MRI and image analysis

MRI was performed on a GE Discovery MR750 3T scanner using a 32 channel hip coil (GE Healthcare, Waukesha, WI, USA) and a 3D balanced steady state gradient-echo pulse sequence (bSSFP) (17,32). In order to reduce banding artifacts, phase-cycling was applied and two images were

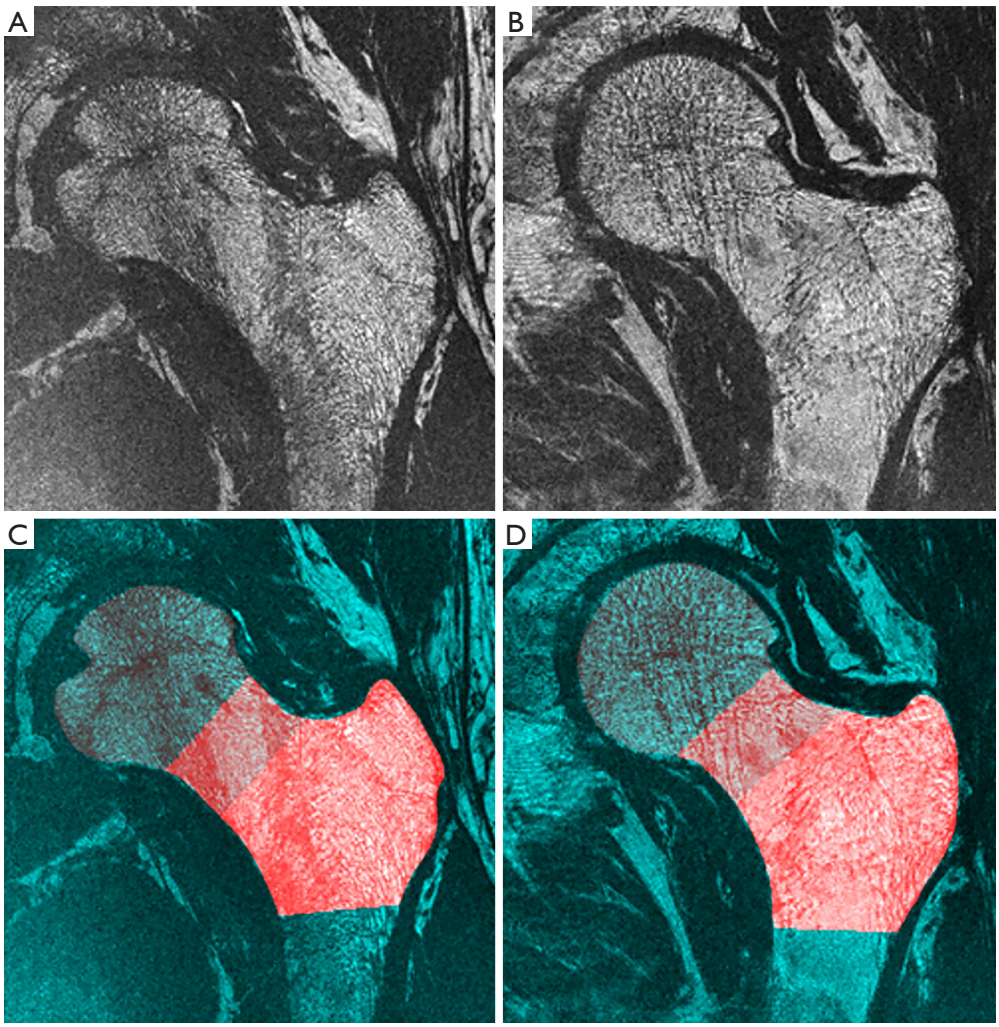

Figure 1 Representative coronal cross-sections of high-resolution magnetic resonance images of the proximal femur of a healthy control (A) and an HIV-infected patient (B) with their corresponding femoral regions highlighted with different shades of red in (C) and (D), respectively: femoral head (dark red), femoral neck (red), and trochanter (bright red).

combined using maximum intensity projection as previously suggested (33). Further parameters included an echo time TE =4.2 ms, readout bandwidth rBW =±62.5 kHz, repetition time TR =10 ms and a flip angle α =60°. A spatial resolution of 234×234×500 μm^3 was achieved in approximately 15 minutes of acquisition time.

Automatic coil correction by nonparametric nonuniform intensity normalization (N3) (24) was applied to all MR scans. The proximal femur was then semi-automatically delineated and the segmentations were used to prescribe three different volumes of interest based on image registration to a common template (30) as depicted in *Figure 1*. The volumes of interest were: femoral head, femoral neck, and trochanter. At each region, local bone enhancement fuzzy clustering (26) was applied to segment the trabecular bone and assess the following four bone parameters: fuzzy bone volume fraction (f-BVF), trabecular number (Tb.N), trabecular spacing (Tb.Sp) and trabecular thickness (Tb.Th), as previously described by Majumdar *et al.* (21).

HR-pQCT imaging and image analysis

All participants were imaged using a clinical HR-pQCT system (Xtreme CT, Scanco Medical AG, Bruttisellen, Switzerland) according to the manufacturer's standard *in vivo* protocols. HR-pQCT images were obtained at the

Table 1 MRI trabecular bone parameters of the femoral head (mean ± SD)

Femoral head	f-BVF	Tb.Th (mm)	Tb.Sp (mm)	Tb.N (1/mm)
HIV-infected	0.384±0.008	0.264±0.009	0.425±0.029	1.454±0.078
Healthy controls	0.392±0.003	0.256±0.006	0.397±0.011	1.532±0.038
P	0.007*	0.031*	0.010*	0.010*

*, significantly different (P<0.05) based on two-tailed unpaired Student's *t*-tests. MRI, magnetic resonance imaging; SD, standard deviation; f-BVF, fuzzy bone volume fraction; Tb.Th, trabecular thickness; Tb.Sp, trabecular separation; Tb.N, trabecular number; HIV, human immunodeficiency virus.

ultradistal radius and ultradistal tibia at 82 μm nominal voxel size in 9.02 mm stack lengths. Bone was segmented using the standard software provided by the manufacturer, and four trabecular bone microstructural parameters were computed: trabecular bone volume fraction (BV/TV), Tb.N, Tb.Th, and trabecular separation (Tb.Sp).

DXA imaging

DXA scans of the lumbar spine (L1 to L3) and the proximal femur (total femur and femoral neck) were obtained using two different scanners (Prodigy, GE/Lunar and Discovery, Hologic), and aBMD was calculated. Online available conversion tables from the manufacturers were used to convert aBMD values between the different scanners.

Statistical analysis

Differences between bone parameters of HIV-infected men and healthy controls were assessed for each imaging modality with two-tailed unpaired Student's *t*-tests as well as with general linear models. The required significance level was set to P<0.05.

Results

Subject characteristics

In the main study, age range for the HIV-infected men spanned 50–69 years [mean ± standard deviation (SD) = 55.5±6.7 years]. BMI range for the HIV-infected men spanned 18–26 kg/m^2 (mean ± SD =23.2±2.7 kg/m^2). Age range for the healthy controls was 52–71 years (mean ± SD =61.5±6.9 years) and BMI was 23–30 kg/m^2 (mean ± SD =26.6±2.5 kg/m^2). Age was not significantly different between groups. However, HIV-infected men had a BMI in the normal range while the control group had a BMI in the overweight range. HIV-infected and control groups had similar distributions of race and ethnicity; in both groups participants were majority White, and each group included two Black participants and one participant of Hispanic descent. Activity level in the HIV-infected individuals met and exceeded the recommendations of the 2008 Physical Activity Guidelines for Americans (US Dept. of Health and Human Services): MET-hours per week for the HIV-infected group spanned 7–39 MET-hours/week (mean ± SD = 17±10 MET-hours/week).

In the ancillary HR-pQCT study, age range for the HIV-infected men spanned 50–69 years (mean ± SD =55.9±6.5 years) and BMI range spanned 18–32 kg/m^2 (mean ± SD = 26.0±3.4 kg/m^2). Age range for the healthy controls was 51–71 years (mean ± SD =58.8±6.1 years) and BMI was 19–34 kg/m^2 (mean ± SD =26.7±3.9 kg/m^2). In this ancillary study, neither age nor BMI was significantly different between groups.

MRI

Results of MRI trabecular bone parameters with means and SDs are summarized in *Table 1* for the femoral head, *Table 2* for the femoral neck, and *Table 3* for the femoral trochanter. In general, parameter values reflected poorer quality of bone microstructure in HIV-infected patients. The pattern of lower BV/TV, lower Tb.N, increased separation, and increased thickness indicates that trabecular bone is lost preferentially by the elimination of thinner trabeculae. *Figure 2* shows examples of the proximal femur MR acquisition along with the individually segmented regions of femoral head, neck, and trochanter in a healthy individual and a HIV-infected subject. In general, all structural bone parameters derived from the femoral head showed significant differences between HIV-infected patients and healthy controls. In the femoral neck, only Tb.Th did not show significant differences. In the femoral trochanter, only Tb.Sp showed significant differences. After adjustment for BMI in the general linear model, all

Table 2 MRI trabecular bone parameters of the femoral neck (mean ± SD)

Femoral neck	f-BVF	Tb.Th (mm)	Tb.Sp (mm)	Tb.N (1/mm)
HIV-infected	0.376±0.012	0.276±0.016	0.460±0.050	1.360±0.117
Healthy controls	0.388±0.008	0.267±0.007	0.422±0.022	1.455±0.057
P	0.024*	0.094	0.037*	0.049*

*, significantly different (P<0.05) based on two-tailed unpaired Student's *t*-tests. MRI, magnetic resonance imaging; SD, standard deviation; f-BVF, fuzzy bone volume fraction; Tb.Th, trabecular thickness; Tb.Sp, trabecular separation; Tb.N, trabecular number; HIV, human immunodeficiency virus.

Table 3 MRI trabecular bone parameters of the femoral trochanter (mean ± SD)

Femoral trochanter	f-BVF	Tb.Th (mm)	Tb.Sp* (mm)	Tb.N (1/mm)
HIV-infected	0.377±0.015	0.281±0.017	0.470±0.057	1.346±0.124
Healthy controls	0.386±0.007	0.269±0.009	0.430±0.024	1.435±0.065
P	0.093	0.063	0.049*	0.059

*, significantly different (P<0.05) based on two-tailed unpaired Student's *t*-tests. MRI, magnetic resonance imaging; SD, standard deviation; f-BVF, fuzzy bone volume fraction; Tb.Th, trabecular thickness; Tb.Sp, trabecular separation; Tb.N, trabecular number; HIV, human immunodeficiency virus.

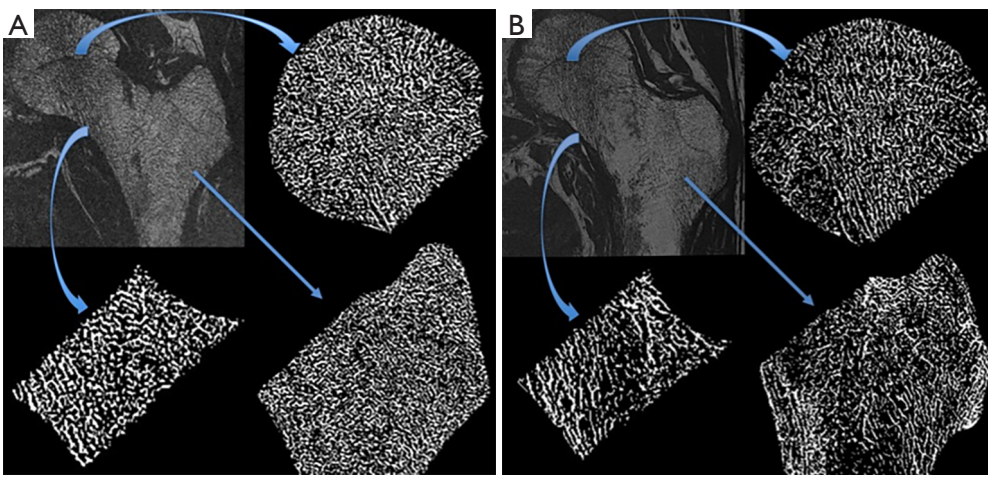

Figure 2 Representative coronal cross-sections of high-resolution magnetic resonance images of the proximal femur of a healthy control (A) and an HIV-infected patient (B) with segmented and thresholded images depicted for each region of interest (head, neck, and trochanter). The HIV-infected patient has relatively lower bone volume fraction, fewer and thicker trabeculae, with greater separation between trabeculae. HIV, human immunodeficiency virus.

significant differences in MRI parameters between groups were attenuated and no longer significant.

HR-pQCT parameters

Results of HR-pQCT trabecular bone parameters for the main study are summarized in *Table 4*. An example of these images is shown in *Figure 3* for a HIV infected patient and a healthy control subject. At the tibia, Tb.N was significantly lower and Tb.Sp was significantly higher in HIV-infected individuals compared to controls, indicative of inferior bone microstructure in HIV-infected patients. At the radius, no significant differences were found between HIV-infected patients and healthy

Table 4 Main study HR-pQCT trabecular bone parameters for ultra-distal tibia

Tibia	BV/TV	Tb.Th (mm)	Tb.Sp (mm)	Tb.N (1/mm)
HIV-infected	0.130±0.021	0.086±0.015	0.593±0.165	1.538±0.295
Healthy controls	0.150±0.022	0.078±0.012	0.444±0.081	1.962±0.308
P	0.061	0.164	0.018*	0.008*

*, significantly different (P<0.05) based on two-tailed unpaired Student's *t*-tests. HR-pQCT, high resolution peripheral quantitative computed tomography; BV/TV, trabecular bone volume fraction; Tb.Th, trabecular thickness; Tb.Sp, trabecular separation; Tb.N, trabecular number; HIV, human immunodeficiency virus.

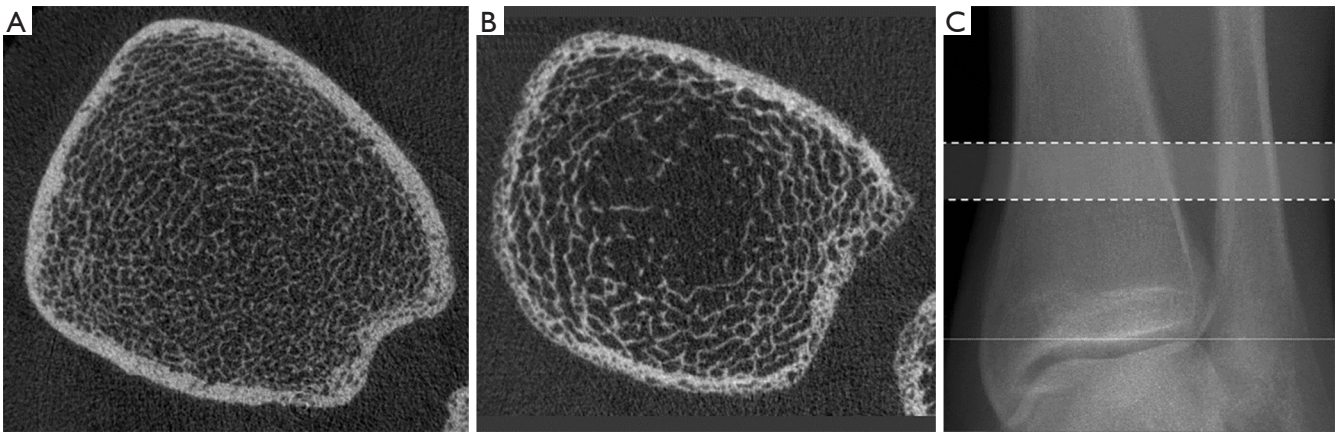

Figure 3 Representative axial cross-sections of HR-pQCT images of the distal tibia of a healthy control (A) and an HIV-infected patient (B). The HIV-infected patient has relatively lower bone volume fraction, fewer and thicker trabeculae, with greater separation between trabeculae. Scout view of the distal tibia depicts the scan region highlighted between dotted lines (C). HR-pQCT, high-resolution peripheral quantitative computed tomography; HIV, human immunodeficiency virus.

Table 5 Ancillary study HR-pQCT trabecular bone parameters for ultra-distal tibia

Tibia	BV/TV	Tb.Th (mm)	Tb.Sp (mm)	Tb.N (1/mm)
HIV-infected	0.143±0.026	0.083±0.013	0.509±0.131	1.756±0.316
Healthy controls	0.161±0.029	0.079±0.009	0.424±0.081	2.034±0.315
P	0.051	0.388	0.023*	0.010*

*, significantly different (P<0.05) based on two-tailed unpaired Student's *t*-tests. HR-pQCT, high resolution peripheral quantitative computed tomography; BV/TV, trabecular bone volume fraction; Tb.Th, trabecular thickness; Tb.Sp, trabecular separation; Tb.N, trabecular number; HIV, human immunodeficiency virus.

controls, however similar trends of inferior bone quality in HIV-infected patients were observed. As with the MRI data, statistical adjustment for BMI in the general linear model eliminated any significant differences in HR-pQCT parameters between groups, suggesting that lower BMI mediates inferior bone microstructure at the tibia in HIV-infected individuals.

Results of HR-pQCT trabecular bone parameters for the ancillary study are summarized in *Table 5*. Just as for the main study, Tb.N was significantly lower and Tb.Sp was significantly higher in HIV-infected individuals compared to controls. In the ancillary study, these microstructural deficits in the HIV-infected men were significant both and the tibia and at the radius (P<0.005).

DXA aBMD

Densitometric results from DXA showed no significant differences between groups for all measurements (lumbar spine and the proximal femur).

Discussion

The goal of this study was to test the hypothesis that trabecular bone microstructure is inferior in HIV-infected men compared to uninfected controls in the central and appendicular skeleton, and compare the results to aBMD derived from DXA measurements, which is the clinical standard for bone health assessment. Using novel image acquisition and analysis approaches, we have found significant impairment in bone microstructure in HIV-infected men, in particular in the distal tibia, femoral head and femoral neck, and to a lesser extent in the femoral trochanter. Areal BMD derived from DXA was not different between HIV-infected men and uninfected controls. These findings underscore the importance of evaluating bone microstructure in addition to aBMD in HIV-infected men.

To the best of our knowledge, only two published studies have investigated bone quality in older HIV-infected individuals (10,11). However, these studies investigated bone quality only at the extremities using HR-pQCT and reported conflicting results. Biver *et al.* (10) found trabecular bone microstructure alterations with lower Tb.N and higher Tb.Sp at the distal radius, as well as lower DXA aBMD at the total femur and ultra-distal radius, in HIV-infected men (median age =64 years) compared to healthy age-, BMI-, and gender-matched controls. In contrast, Yin *et al.* (11) did not find significant differences in structural HR-pQCT parameters of trabecular bone at the distal radius and distal tibia between HIV-infected women (mean age =58 years) and uninfected controls, but found lower DXA aBMD at the spine, total hip and ultradistal radius in HIV-infected women.

In our main study, HIV-infected and uninfected control men had a small but significant difference in BMI. Statistical adjustment for BMI using general linear models eliminated significant differences in microstructure between groups. This may indicate that BMI is solely responsible for differences in bone quality between groups, or that lower BMI, an established co-morbidity of HIV infection, may mediate the development of poor bone microstructure in HIV-infected patients. To investigate whether differences in BMI alone account for the bone quality differences found in the main study, we performed an ancillary HR-pQCT study of 20 HIV-infected men and 18 age- and BMI-matched uninfected controls. The results of this ancillary study reflect the HR-pQCT results of the main study, with the additional finding of significant differences in the radius parameters. This supports our hypothesis that HIV status, regardless of BMI, impact trabecular bone quality in older men.

This study used high-resolution MRI to quantify trabecular bone parameters at the proximal femur and HR-pQCT to quantify trabecular bone parameters at the radius and tibia. Though these imaging modalities differ in many important ways in both acquisition and analysis protocols, previously published results document good correlations between the two methods (34,35).

A limitation of our study is the sample size. With the limited sample size we may not be powered to detect aBMD differences between HIV-infected subjects and healthy controls as reported in previous studies in the literature. Importantly, our data show that even with the small sample size, we were able to detect differences in trabecular microstructure using high resolution imaging techniques. Furthermore, the trabecular bone impairment which was most significant in the femoral head might be attributable to AVN which is prevalent in HIV infected subjects (4,5). However, we do not have conclusive evidence of AVN in these subjects.

In conclusion, we have identified impaired trabecular bone microstructure in HIV-infected men compared to uninfected controls, while DXA detected no significant differences between groups. We also found that these differences were more pronounced in the femoral head. This initial study highlights the relevance of MRI and HR-pQCT as powerful and necessary imaging tools in the assessment of bone health in this population. Larger-cohort studies incorporating these advanced imaging tools are needed.

Acknowledgements

Funding: NIH R01AI125080, NIH R01-AR057336, NIH P30-AI027763 (UCSF Gladstone Institute of Virology & Immunology Center for AIDS Research).

Footnote

Conflicts of Interest: The authors have no conflicts of interest to declare.

Ethnical Statement: The study was conducted in accordance with the Committee for Human Research at our institution and followed all regulations. Informed consent was obtained before scans.

References

1. Ofotokun I, Weitzmann MN. HIV and bone metabolism. Discov Med 2011;11:385-93.
2. Ofotokun I, Weitzmann MN. HIV-1 infection and antiretroviral therapies: risk factors for osteoporosis and bone fracture. Curr Opin Endocrinol Diabetes Obes 2010;17:523-9.
3. Hoy J, Young B. Do people with HIV infection have a higher risk of fracture compared with those without HIV infection? Curr Opin HIV AIDS 2016;11:301-5.
4. Matos MA, Alencar RW, Matos SS. Avascular necrosis of the femoral head in HIV infected patients. Braz J Infect Dis 2007;11:31-4.
5. Chevalier X, Larget-Piet B, Hernigou P, Gherardi R. Avascular necrosis of the femoral head in HIV-infected patients. J Bone Joint Surg Br 1993;75:160.
6. Blake GM, Fogelman I. The role of DXA bone density scans in the diagnosis and treatment of osteoporosis. Postgrad Med J 2007;83:509-17.
7. Genant HK, Engelke K, Prevrhal S. Advanced CT bone imaging in osteoporosis. Rheumatology (Oxford) 2008;47 Suppl 4:iv9-16.
8. Prior J, Burdge D, Maan E, Milner R, Hankins C, Klein M, Walmsley S. Fragility fractures and bone mineral density in HIV positive women: a case-control population-based study. Osteoporos Int 2007;18:1345-53.
9. McComsey GA, Huang JS, Woolley IJ, Young B, Sax PE, Gerber M, Swindells S, Bonilla H, Gopalakrishnan G. Fragility fractures in HIV-infected patients: need for better understanding of diagnosis and management. J Int Assoc Physicians AIDS Care (Chic) 2004;3:86-91.
10. Biver E, Calmy A, Delhumeau C, Durosier C, Zawadynski S, Rizzoli R. Microstructural alterations of trabecular and cortical bone in long-term HIV-infected elderly men on successful antiretroviral therapy. AIDS 2014;28:2417-27.
11. Yin MT, Shu A, Zhang CA, Boutroy S, McMahon DJ, Ferris DC, Colon I, Shane E. Trabecular and cortical microarchitecture in postmenopausal HIV-infected women. Calcif Tissue Int 2013;92:557-65.
12. Cooper C, Atkinson EJ, Jacobsen SJ, O'Fallon WM, Melton LJ 3rd. Population-based study of survival after osteoporotic fractures. Am J Epidemiol 1993;137:1001-5.
13. Yin MT, Zhang CA, McMahon DJ, Ferris DC, Irani D, Colon I, Cremers S, Shane E. Higher rates of bone loss in postmenopausal HIV-infected women: a longitudinal study. J Clin Endocrinol Metab 2012;97:554-62.
14. Young B, Dao CN, Buchacz K, Baker R, Brooks JT; HIV Outpatient Study (HOPS) Investigators. Increased rates of bone fracture among HIV-infected persons in the HIV Outpatient Study (HOPS) compared with the US general population, 2000-2006. Clin Infect Dis 2011;52:1061-8.
15. Gallant JE, Staszewski S, Pozniak AL, DeJesus E, Suleiman JM, Miller MD, Coakley DF, Lu B, Toole JJ, Cheng AK; 903 Study Group. Efficacy and safety of tenofovir DF vs stavudine in combination therapy in antiretroviral-naive patients: a 3-year randomized trial. JAMA 2004;292:191-201.
16. McComsey GA, Tebas P, Shane E, Yin MT, Overton ET, Huang JS, Aldrovandi GM, Cardoso SW, Santana JL, Brown TT. Bone disease in HIV infection: a practical review and recommendations for HIV care providers. Clin Infect Dis 2010;51:937-46.
17. Krug R, Banerjee S, Han ET, Newitt DC, Link TM, Majumdar S. Feasibility of in vivo structural analysis of high-resolution magnetic resonance images of the proximal femur. Osteoporos Int 2005;16:1307-14.
18. Han M, Chiba K, Banerjee S, Carballido-Gamio J, Krug R. Variable flip angle three-dimensional fast spin-echo sequence combined with outer volume suppression for imaging trabecular bone structure of the proximal femur. J Magn Reson Imaging 2015;41:1300-10.
19. Krug R, Burghardt AJ, Majumdar S, Link TM. High-resolution imaging techniques for the assessment of osteoporosis. Radiol Clin North Am 2010;48:601-21.
20. Wehrli FW, Hwang SN, Song HK, Gomberg BR. Visualization and analysis of trabecular bone architecture in the limited spatial resolution regime of in vivo micro-MRI. Adv Exp Med Biol 2001;496:153-64.
21. Majumdar S, Genant HK. Assessment of trabecular structure using high resolution magnetic resonance imaging. Stud Health Technol Inform 1997;40:81-96.
22. Majumdar S, Kothari M, Augat P, Newitt DC, Link TM, Lin JC, Lang T, Lu Y, Genant HK. High-resolution magnetic resonance imaging: three-dimensional trabecular bone architecture and biomechanical properties. Bone 1998;22:445-54.
23. Wehrli FW, Ford JC, Haddad JG. Osteoporosis: clinical assessment with quantitative MR imaging in diagnosis. Radiology 1995;196:631-41.
24. Folkesson J, Krug R, Goldenstein J, Issever AS, Fang C, Link TM, Majumdar S. Evaluation of correction methods

for coil-induced intensity inhomogeneities and their influence on trabecular bone structure parameters from MR images. Med Phys 2009;36:1267-74.
25. Carballido-Gamio J, Phan C, Link TM, Majumdar S. Characterization of trabecular bone structure from high-resolution magnetic resonance images using fuzzy logic. Magn Reson Imaging 2006;24:1023-9.
26. Folkesson J, Carballido-Gamio J, Eckstein F, Link TM, Majumdar S. Local bone enhancement fuzzy clustering for segmentation of MR trabecular bone images. Med Phys 2010;37:295-302.
27. Saha PK, Wehrli FW. Measurement of trabecular bone thickness in the limited resolution regime of in vivo MRI by fuzzy distance transform. IEEE Trans Med Imaging 2004;23:53-62.
28. Wehrli FW, Saha PK, Gomberg BR, Song HK, Snyder PJ, Benito M, Wright A, Weening R. Role of magnetic resonance for assessing structure and function of trabecular bone. Top Magn Reson Imaging 2002;13:335-55.
29. Carballido-Gamio J, Folkesson J, Karampinos DC, Baum T, Link TM, Majumdar S, Krug R. Generation of an atlas of the proximal femur and its application to trabecular bone analysis. Magn Reson Med 2011;66:1181-91.
30. Carballido-Gamio J, Bonaretti S, Saeed I, Harnish R, Recker R, Burghardt AJ, Keyak JH, Harris T, Khosla S, Lang TF. Automatic multi-parametric quantification of the proximal femur with quantitative computed tomography. Quant Imaging Med Surg 2015;5:552-68.
31. Stewart AL, Mills KM, King AC, Haskell WL, Gillis D, Ritter PL. CHAMPS physical activity questionnaire for older adults: outcomes for interventions. Med Sci Sports Exerc 2001;33:1126-41.
32. Banerjee S, Han ET, Krug R, Newitt DC, Majumdar S. Application of refocused steady-state free-precession methods at 1.5 and 3 T to in vivo high-resolution MRI of trabecular bone: simulations and experiments. J Magn Reson Imaging 2005;21:818-25.
33. Bangerter NK, Hargreaves BA, Vasanawala SS, Pauly JM, Gold GE, Nishimura DG. Analysis of multiple-acquisition SSFP. Magn Reson Med 2004;51:1038-47.
34. Krug R, Carballido-Gamio J, Burghardt AJ, Kazakia G, Hyun BH, Jobke B, Banerjee S, Huber M, Link TM, Majumdar S. Assessment of trabecular bone structure comparing magnetic resonance imaging at 3 Tesla with high-resolution peripheral quantitative computed tomography ex vivo and in vivo. Osteoporos Int 2008;19:653-61.
35. Kazakia GJ, Hyun B, Burghardt AJ, Krug R, Newitt DC, de Papp AE, Link TM, Majumdar S. In vivo determination of bone structure in postmenopausal women: a comparison of HR-pQCT and high-field MR imaging. J Bone Miner Res 2008;23:463-74.

Cite this article as: Kazakia GJ, Carballido-Gamio J, Lai A, Nardo L, Facchetti L, Pasco C, Zhang CA, Han M, Parrott AH, Tien P, Krug R. Trabecular bone microstructure is impaired in the proximal femur of human immunodeficiency virus-infected men with normal bone mineral density. Quant Imaging Med Surg 2018;8(1):5-13. doi: 10.21037/qims.2017.10.10

